Research Square

Preprints are preliminary reports that have not undergone peer review.
They should not be considered conclusive, used to inform clinical practice,
or referenced by the media as validated information.

Adsorption of Selected Monovalent and Divalent Metal Ions from Anwai River Using Chitosan Derived from Crab Shells: Efficiency and Kinetic Evaluation

Vincent Oshevwiyo Akpoveta

akpoveta.oshevwiyo@dou.edu.ng

Dennis Osadebay University

Prosper Etoh
Dennis Osadebay University

Prosper Chinyelum Okwuenu
Dennis Osadebay University

Elvis Ebubechukwu Okocha
Dennis Osadebay University

Sophia Isioma Nwabuzor
Dennis Osadebay University

Praise Oghenevwegba Umukoro
Dennis Osadebay University

Ese Queen Umudi
University of Delta

Clara Ogbebor Ekwe
State University of Medical and Applied Science, Igbo-Eno

Bright Aiyehirue Agwogie
Dennis Osadebay University

Andrew Onofuevure
Dennis Osadebay University

Apuyor Stanley
Dennis Osadebay University

Apuyor Kingsley
Dennis Osadebay University

Joe Ejohwomu Otovbo
Dennis Osadebay University

Onome Edigbina
Dennis Osadebay University

John Arigbede
University of Massachusetts

Kingsley Imoni-Ogbe
University of Delta

Wesley Okiei
University of Lagos

Praise Samuel Ezeagwu

Research Article

Keywords: Chitosan, crab shell, Anwai River, monovalent ions, divalent ions, adsorption kinetics, biosorbent

Posted Date: October 27th, 2026

DOI: https://doi.org/10.21203/rs.3.rs-11340713/v1

License: This work is licensed under a Creative Commons Attribution 4.0 International License. Read Full License

Additional Declarations: No competing interests reported.

Abstract

Crustacean-shell-derived chitosan is a renewable biopolymer containing amino and hydroxyl groups capable of interacting with dissolved metal ions. This study evaluated chitosan prepared from crab-shell waste for removing selected monovalent and divalent metal ions from Anwai River water, Delta State, Nigeria. Crab shells obtained from Pessu Market, Warri, Delta State, were subjected to demineralization, deproteinization, and alkaline deacetylation to obtain Chitosan and the product was characterized by Fourier-transform infrared spectroscopy (FTIR). FTIR evidence indicated conversion of chitin to chitosan, with attenuation and shifts of amide-related bands following deacetylation. A Chitosan bed packed column was used to treat the bulk river water, with effluent collected at 0, 20, 40, 60, 80, and 100 min. River water samples were analyzed by atomic absorption spectrophotometry for the selected monovalent and divalent metal ions (Na, K, Li, Ag, Mg, and Mn). Initial concentrations were 0.614, 6.197, 0.184, 0.085, 0.051, and 0.173 mg L^{-1} for Mg, Na, K, Li, Ag, and Mn, respectively. Maximum reported removal efficiencies were 3.10% for Mg, 84.91% for Na, 76.09% for K, 56.47% for Li, 21.57% for Ag and 84.39% for Mn. Elovich gave the highest R^2 values for Mg (0.4107), Na (0.3621), Li (0.9503), and Mn (0.8822), whereas pseudo-second-order gave the highest R^2 values for K (0.5513) and Ag (0.7654). Several fitted parameters were physically unrealistic or associated with low R^2 values; therefore, the kinetic fits is not interpreted as definitive mechanistic proof, which indicates that further controlled batch and column studies are required before scale-up. The findings demonstrate that crab-shell-derived chitosan is a promising, eco-friendly, and cost-effective biosorbent for the removal of selected metal ions from river water, while supporting further investigation through replicated equilibrium and controlled column experiments to establish its adsorption performance and practical applicability.

1. Introduction

Freshwater quality is increasingly affected by anthropogenic activities, and dissolved metals are among the contaminants requiring effective control because of their persistence and potential for bioaccumulation. Anthropogenic activities arising from industrial activities, domestic wastes, mining, and agricultural runoff may serve as plausible contributors to metal contamination of the Anwai River, which can introduce potentially toxic metals into associated rivers and other receiving water bodies, because of the strategic location of the River in the highly urbanized State capital city, thereby creating environmental concerns. Such contamination of freshwater by dissolved metals creates a need for inexpensive and locally available treatment materials. Conventional treatment processes, including precipitation, ion exchange, and membrane separation, can be effective for metal-contaminated water treatment but may involve relatively high operational costs, chemical consumption, or process complexity [1–3]. Although such conventional remediation practices may be effective under appropriate conditions, these approaches can be associated with relatively high operating costs, sludge generation, membrane fouling, or other limitations. Adsorption is therefore widely investigated as a comparatively simple treatment approach, particularly where low-cost and renewable sorbents are available [3, 4].

Chitosan is a partially deacetylated derivative of chitin, a structural polysaccharide abundant in crustacean shells. Its structure contains amino and hydroxyl groups that can participate in coordination, ion exchange, and other interactions with dissolved metal ions [5–8]. The production of chitosan from seafood-processing residues also provides a route for converting biological waste into a value-added material [6, 7]. Reviews of chitosan-based adsorbents have emphasized the importance of adsorbent structure, pH, competing ions, contact time, and kinetic behavior in determining treatment performance [9–11].

Crab shells are attractive feedstocks because their chitin can be isolated by sequential demineralization and deproteinization and converted to chitosan by alkaline deacetylation [6, 7, 12]. Previous work has demonstrated metal uptake by crab-shell-derived chitosan and identified pore diffusion and surface interactions as possible contributors to uptake [13]. However, many adsorption studies use single-metal synthetic solutions, whereas river water contains multiple ions and a more complex matrix.

Anwai River in Delta State, Nigeria, is a small surface-water system used by surrounding communities. This study investigated the application of locally prepared crab-shell chitosan to a spatially composite Anwai River-water sample. The objectives were to prepare and characterize chitosan from crab shells, determine selected Mg, Na, K, Li, Ag, and Mn concentrations, evaluate their removal during column treatment, and compare different adsorption kinetic protocols such as pseudo-first-order, pseudo-second-order, intraparticle-diffusion, and the Elovich model to ascertain its metal adsorption kinetic descriptions.

2. Materials and Methods

2.1 Study area and sampling

Crab shells were obtained from Pessu Market, Warri, in Warri South Local Government Area, Delta State, Nigeria. River water was collected from Anwai River within Oshimili South Local Government Area, Asaba, Delta State, Nigeria, at approximately 6°15'18" N latitude and 6°41'26" E longitude (Fig. 1). Six grab samples were collected at locations separated by distances of approximately 20 m and combined in a clean 4-L container to form a spatial composite sample.

2.2 Preparation of chitosan

Crab shells were washed, sun-dried, crushed, and oven-dried at approximately 102°C for 5 h before grinding. The ground material was demineralized with 0.85 M HCl for 6 h. The demineralized material was treated with concentrated NaOH at a shell-to-solution ratio of 1:2.5 at 0°C for 18 h for deproteinization, followed by treatment with 1 M HCl at 90°C for 12 h. 30 g of the resulting chitin was mixed with 40% (w/v) NaOH and 150 mL 2-propanol and refluxed for 2 h to achieve deacetylation. The product was washed to neutral pH, treated with 5% EDTA, washed again, and dried at 60°C to constant mass. These operations follow established crustacean chitin/chitosan preparation sequences [6, 7, 12].

2.3 FTIR characterization

Chitin and prepared chitosan were characterized using an Agilent Cary 630 FTIR spectrometer over 4000–650 cm − 1 at a reported resolution of 8 cm^{-1}. Spectra were used to assess changes in O–H, N–H, C–H, amide, and C–O-related bands.

2.4 Column adsorption experiment

A mass of 2.56 g chitosan was packed into a burette and retained with a small quantity of wool. A 50 mL aliquot of composite river water was introduced into the column. The first flow-through was collected at 0 min, followed by subsequent effluent collection at 20, 40, 60, 80, and 100 min. Samples were analyzed for Mg, Na, K, Li, Ag, and Mn using a 240FS AA Agilent Technologies atomic absorption spectrophotometer.

2.5 Digestion and AAS analysis

50 mL of each sample was mixed with 1 mL nitric acid and heated at 100°C until boiling. After cooling, the sample was filtered through Whatman filter paper and retained for AAS analysis.

2.6 Adsorption calculations and kinetic models

Adsorption capacity was calculated as $q_t = (C_0 - C_t)V$

m

where qt is adsorption capacity (mg g − 1),

C0 is initial concentration (mg L − 1),

Ct is concentration at time t,

V is solution volume (L), and

M is adsorbent mass (g).

Removal efficiency was calculated as Removal Efficiency (%) = $\frac{C0-Ct}{C0} \times 100$.

Pseudo-first-order, pseudo-second-order, intraparticle-diffusion, and Elovich models were evaluated using the linearized forms of their respective models. The pseudo-first-order model was evaluated from the linear relationship between $\ln(q_e-q_t)$ and t; the pseudo-second-order model from t/q_t versus t; the intraparticle-diffusion model from q_t versus $t^{0.5}$; and the Elovich model from q_t versus ln(t). The highest R^2 was used as the statistical best fit, but interpretation was additionally constrained by physical plausibility of fitted parameters.

2.7 Comparison with drinking-water guidelines

Measured metal concentrations were compared with the applicable current drinking-water guideline values and the relevant edition of the Nigerian Standard for Drinking Water Quality.

3. Results and Discussion

3.1 Physical characteristics of chitosan extracted from crab shells

Figure 2. Physical appearance of chitosan extracted from crab shells.

The crab shell-derived chitosan material shown in Fig. 2 above appears as a brown to light-brown, finely powdered solid with a predominantly granular texture and several small, irregular agglomerates. Its surface appears relatively uniform in colour, although some coarser particles are visible. These features provide a descriptive account of the recovered material's macroscopic appearance. The brown coloration may indicate the persistence of shell-derived pigments or other residual impurities following extraction, although colour alone cannot establish their presence. The final appearance of crab-shell chitosan can vary with the crab species, demineralization and deproteinization efficiency, the extent of chitin deacetylation, and any subsequent washing or decolourization treatments. Recent research on chitosan from crab shells confirms that extraction conditions influence important physicochemical properties, including degree of deacetylation, ash content, and crystallinity [14].

This physical appearance cannot alone qualitatively confirm the chemical identity of the extracted material as chitosan, therefore necessitating further characterization using Fourier-transform infrared spectroscopy (FTIR) to help verify the characteristic functional groups associated with a well-extracted chitosan material, as this will provide complementary evidence of material characteristics and quality [14. 15].

3.1 FTIR characterization

The FTIR spectra's of chitin and chitosan isolated from crab shell are presented in Figs. 2 and 3, respectively, below.

An examination of these two spectra indicates that chitin has been effectively deacetylated to form chitosan. The chitin spectrum in Fig. 2 showed an O–H stretching band at 3439.04 cm^{-1}, comparable to the standard absorption band at 3448 cm^{-1}, and N–H-related bands at approximately 3253 and 3100 cm^{-1}, which closely aligned with the previously reported values of 3253 cm^{-1} and 3107 cm^{-1} for α-chitin [16]. Notably, these bands were significantly diminished in chitosan, as depicted in Fig. 3. After deacetylation, these bands were attenuated. A C–H band occurred at 2874.82 cm^{-1} (Fig. 2), while bands at 1661 and 1619 cm^{-1} in chitin decreased in intensity and shifted to approximately 1639.65 and 1583.07 cm^{-1} in the chitosan product (Fig. 3). The band intensity at 1651 cm^{-1} (Fig. 2), corresponding to the stretching of C = O and C-O-NH in the amide of chitin, was found to decrease in chitosan and shifted to 1639.65 cm^{-1} (Fig. 3). The absorption bands associated with the amide group and CH stretching in chitin were identified at 1428.46 cm^{-1} and 1375.13 cm^{-1}, respectively

(Fig. 2), but shifted to approximately 1400 cm^{-1} in chitosan (Fig. 3). Additional bands around 1076 and 1055 cm^{-1} were assigned to C–O stretching, while the absorption observed within the range of 1349 to 1421 cm^{-1} is attributable to the amide groups present in the glucosamine structure [17]. The attenuation of amide-related bands is consistent with conversion of chitin to chitosan and increased availability of amino groups for metal binding [5, 6, 8]. The degree of deacetylation was not independently quantified; therefore, the FTIR evidence should be regarded as qualitative characterization, rather than a numerical determination of degree of deacetylation.

3.2 Metal concentrations and removal performance

Table 1
Concentrations of selected metals in the composite Anwai River sample and column effluent.

Time (min)	Mg (mg L^{-1})	Na (mg L^{-1})	K (mg L^{-1})	Li (mg L^{-1})	Ag (mg L^{-1})	Mn (mg L^{-1})
0	0.630 ± 0.045	0.935 ± 0.065	0.106 ± 0.098	0.217 ± 0.067	0.031 ± 0.016	0.027 ± 0.035
20	0.655 ± 0.063	1.470 ± 0.081	0.044 ± 0.016	0.076 ± 0.004	0.030 ± 0.021	0.069 ± 0.008
40	0.595 ± 0.054	9.585 ± 0.053	0.110 ± 0.035	0.094 ± 0.008	0.038 ± 0.009	0.055 ± 0.064
60	0.714 ± 0.123	9.883 ± 0.005	0.064 ± 0.021	0.044 ± 0.002	0.038 ± 0.004	0.0295 ± 0.018
80	0.661 ± 0.065	9.395 ± 0.546	0.084 ± 0.013	0.047 ± 0.004	0.023 ± 0.001	0.105 ± 0.019
100	0.679 ± 0.047	3.050 ± 0.263	0.203 ± 0.019	0.037 ± 0.004	0.040 ± 0.006	0.115 ± 0.010
Initial	0.614 ± 0.074	6.197 ± 3.913	0.184 ± 0.009	0.085 ± 0.011	0.051 ± 0.017	0.173 ± 0.132

The reported initial concentrations of the investigated monovalent and divalent metal ions in Anwai River water samples were 0.614 ± 0.074 mg L^{-1}, 6.197 ± 3.913 mg L^{-1}, 0.184 ± 0.009 mg L^{-1}, 0.085 ± 0.011 mg L^{-1}, 0.051 ± 0.017 mg L^{-1} and 0.173 ± 0.132 mg L^{-1} for Mg, Na, K, Li, Ag and Mn, respectively, as seen in Table 1. The maximum removal efficiencies were calculated as 3.10% for Mg, 84.91% for Na, 76.09% for K, 56.47% for Li, 21.57% for Ag, and 84.39% for Mn (Table 1).

The concentrations of the divalent metals in Anwai River water were relatively low, with initial concentrations of approximately 0.173 mg L^{-1} for Mn and 0.614 mg L^{-1} for Mg. Following treatment with the chitosan-based adsorbent, the residual metal concentrations varied across the contact times investigated. The highest removal efficiency for Mn was 84.39% at 0 min, whereas Mg exhibited a maximum removal efficiency of only 3.10% at 40 min (Table 1). The markedly higher removal of Mn compared with Mg indicates a greater affinity of the chitosan-based adsorbent for Mn under the experimental conditions, while the limited removal of Mg suggests weaker adsorbent–metal interactions.

The initial concentrations of the monovalent metals were also relatively low (6.197 mg L^{-1} Na, 0.184 mg L^{-1} K, 0.085 mg L^{-1} Li, and 0.051 mg L^{-1} Ag), as seen in Table 1. Na occurred at the highest concentration among these metals, whereas Ag had the lowest. The maximum removal efficiencies were 84.91% for Na at 0 min, 76.09% for K at 20 min, 56.47% for Li at 100 min, and 21.17% for Ag at 80 min. These results indicate that the chitosan-based adsorbent exhibited greater removal efficiency toward Na, K, and Li than toward Ag under the conditions studied.

Their removal efficiencies did not exhibit a consistent temporal trend. Some metals showed the highest removal at the initial contact time rather than after prolonged exposure, while others showed maximum removal at later contact times. This irregular pattern suggests that adsorption was influenced by metal-specific interactions with the available binding sites rather than by contact time alone. The absence of a progressive increase in removal efficiency with increasing contact time may also indicate rapid occupation of readily accessible adsorption sites, followed by slower mass transfer and/or partial saturation of the available binding sites. Consequently, contact time did not exert a uniform influence on metal removal across the investigated metals. The observed higher metal concentrations in the Chitosan treated effluent as

against their initial concentrations as seen in the metals, with the exception of Ag and Mn, could be due to minute leaching of these metals (Mg, Na, K, Li) from the Chitosan biosorbent at prolonged contact time.

Non-monotonic profiles, rather than a continuous decline, can also arise in flow-through systems from transient mass transfer, preferential retention, desorption, channeling, matrix effects, or analytical variability. Importantly, the 0-min value represents the first column effluent rather than a separately analyzed untreated influent; therefore, the reported maximum removal efficiencies should not be interpreted as equilibrium capacities. Chitosan contains amino and hydroxyl groups capable of metal coordination and ion exchange, but ion-specific affinity depends on charge, hydration, competing ions, and solution chemistry [8–11]. The present experiment does not provide sufficient controlled information on pH, ionic strength, or competing ions to establish individual mechanisms conclusively, which could therefore be the basis for future studies.

The measured concentrations of Na (6.20 mg L^{-1}), Li (0.08 mg L^{-1}), Mg (0.614 mg L^{-1}), Ag (0.05 mg L^{-1}), K (0.184 mg L^{-1}) and Mn (0.173 mg L^{-1}) were compared with applicable drinking-water standards. The Na concentration was substantially below the 200 mg L^{-1} value adopted by WHO as an acceptability threshold and as the maximum permitted concentration under the Nigerian Standard for Drinking Water Quality [18, 19], and was therefore considered safe. The Ag concentration was below the WHO provisional reference value of 0.10 mg L^{-1} [18], thus constituting no health risk.

The Mg concentration exceeded the SON maximum permitted level of 0.20 mg L^{-1} [13], while Mn exceeded the WHO provisional reference value of 0.08 mg L^{-1} [18], but remained within the SON range of 0.20 mg L^{-1} [19]. No specific WHO health-based guideline value or SON maximum permissible limit is currently specified for Li and K. However, potassium concentration was found to be below the reported permissible/assessment value of 1.5 mg L^{-1} in some water-quality standards [20, 21]. Lithium concentrations were evaluated against a non-regulatory Health-Based Screening Level (HBSL) of 0.01 mg/L (10 µg/L), as reported [22, 23]. A lithium concentration of 0.01 mg L^{-1} adopted as a health-based screening benchmark, consistent with the USGS/EPA Health-Based Screening Level reported by Lindsey et al. [22] and subsequent drinking water occurrence studies [23], was found to be above the reported lithium concentration in Anwai River. Mg, Mn, and Li are therefore of environmental concern, requiring ongoing monitoring and possible mitigation measures to reduce excessive exposure for the local population that relies on the River water for domestic purposes.

3.3 Kinetic modelling

Adsorption kinetics was evaluated for all the metals using pseudo-First order, pseudo-Second order, Intraparticle diffusion and Elovich models.

Table 2
Summary of reported kinetic parameters.

Metal	PFO k_1 (min^{-1})	PFO R^2	PSO k_2($gmg^{-1}min^{-1}$)	PSO R^2	Int-P Diff K_{id} ($mgg^{-1}min^{-0.5}$)	Int-P Diff R^2	Elovich α ($mg\ g^{-1}\ min^{-1}$); β ($g\ mg^{-1}$)	Elovich R^2	Highest R^2
Mg	32.64	0.2978	0.0002	0.2559	0.0002	0.2559	α: 9.15×10^{-7}; β: 2258.26	0.4107	0.4107 (Elovich)
Na	0.0032	0.0035	−0.0611	0.0316	-0.013	0.3119	α: -8.16×10^{-4}; β: −33.51	0.3621	0.3621 (Elovich)
K	−0.0156	0.0251	2.52×10^{-3}	0.5513	-0.0001	0.1223	α: 8.32×10^{-12}; β: −7692.31	0.06	0.5513 (PSO)
Li	0.0185	0.0234	0.0067	0.0003	0.0003	0.8767	α: 2.77×10^{-5}; β: 1320	0.9503	0.9503 (Elovich)
Ag	−0.0435	0.2235	−917.3	0.7654	-7×10^{-6}	0.0450	α: -4.46×10^{-16}; β: -6.10×10^{4}	0.0485	0.7654 (PSO)
Mn	−386.66	0.8073	-3.63×10^{-4}	0.4322	-0.0033	0.7004	α: -1.05×10^{-4}; β: −126.30	0.8822	0.8822 (Elovich)

PFO = pseudo-first-order; PSO = pseudo-second-order; Int-P Diff = intraparticle diffusion model

Elovich gave the highest R^2 for Mg (0.4107), Na (0.3621), Li (0.9503), and Mn (0.8822), whereas pseudo-second-order gave the highest R^2 for K (0.5513) and Ag (0.7654), as seen in Table 2. Model comparisons of this type are common in chitosan adsorption studies [9, 10]. However, R^2 alone is insufficient for assigning a mechanism, particularly when concentration profiles are non-monotonic or fitted parameters are physically unrealistic.

The comparatively strong Elovich fit for Li (R^2 = 0.9503) provides an empirical description of the observed temporal response, but does not by itself prove chemisorption. The Mn Elovich fit (R^2 = 0.8822) likewise has a comparatively high R^2, yet the reported α and β values are negative and therefore physically inconsistent with their conventional meanings. The reported pseudo-second-order rate constant for Ag is also negative (− 917.3 g mg − 1 min − 1), which is not physically meaningful. Thus, the kinetic results are interpreted cautiously as statistical comparisons rather than definitive evidence of the adsorption mechanism.

Mg and Na showed low R^2 values across the models, indicating that none of the tested linearized equations adequately represented their temporal profiles.

3.4 Practical implications

The study demonstrates a potentially useful route for converting crab-shell waste into a functional biosorbent. Chitosan is renewable and contains reactive amino and hydroxyl groups, while shell-derived production contributes to waste valorization. However, the present findings will not be interpreted as generalized proof that treated water meets drinking-water standards because only selected metals were examined, the sampling represented one composite event, and equilibrium and long-term column performance were not established.

4. Conclusions

Chitosan was prepared from crab shells through demineralization, deproteinization, and alkaline deacetylation, and FTIR spectra showed changes consistent with conversion of chitin to chitosan. The chitosan column produced maximum reported reductions for Na, K, Li and Mn, while Mg and Ag showed lower reductions. Elovich gave the highest R^2 for Mg, Na, Li and Mn, whereas pseudo-second-order gave the highest R^2 for K and Ag. Because the concentration profiles were non-monotonic and several fitted parameters were physically invalid, the kinetic fits should be treated as empirical rather than definitive mechanistic evidence. Replicated controlled column and equilibrium studies are required before practical treatment claims are made. The study supports further investigation of crab-shell-derived chitosan as a low-cost biosorbent for selected metals removal from River water, while emphasizing the need for better-controlled adsorption experiments before practical application. Elevated levels of some metals investigated raise serious environmental concern about the health and safety of the local population around Anwai River, necessitating monitoring and mitigating interventions.

5. Recommendations

Continued monitoring of lithium, manganese, and magnesium concentrations in the Anwai River is recommended, as these metals were identified as constituents of environmental concern that warrant further assessment. Future investigations should also evaluate additional and more comprehensive kinetic models for metals that exhibited poor fits to the four models considered in the present study. Further research should examine the effects of chitosan modification, solution pH, adsorbent dosage, and hydraulic flow rate on metal-ion removal performance. In addition, equilibrium isotherm studies should be conducted to establish adsorption capacity and elucidate the underlying adsorption mechanisms. Studies on adsorbent regeneration and reuse are also recommended to assess the practical sustainability and economic feasibility of chitosan-based treatment. Finally, post-adsorption surface characterization should be undertaken to provide further insight into the physicochemical interactions and mechanisms responsible for metal-ion uptake.

Declarations

Conflict of interest

The authors declare no conflict of interest.

Ethical approval

Not applicable to the reported laboratory study.

Consent to participate

Not applicable.

Consent for publication

Not applicable.

Third party material

Authors have declared that all of the material in the manuscript is owned by the authors and/or no permissions are required.

Funding

No external funding was received.

Author Contribution

Author contributionsV.O.A, P.O, P.C.O, and W.O. were involved in Conceptualization; Methodology, E.E.O, S.I.N, P.O.U, and P.S.E were involved in Methodology; K.I.O and V.O.A. were involved in software; V.O.A., C.O.E, E.Q.U and K.I.O were involved in validation; V.O.A, B.A.A and C.O.E. were involved in formal analysis; W.O, V.O.A, E.E.O, S.I.N, P.O.U, and P.S.E were involved in investigation; E.Q.U, J.A. provided resources; V.O.A and K.I.O were involved in data curation; W.O, P.O, P.C.O and V.O.A. were involved in Writing—original draft preparation; V.O.A., E.Q.U and C.O.E were involved in Writing—review and editing; K.I.O, V.O.A and E.Q.U were involved in visualization; V.O.A, W.O, P.O, and P.C.O were involved in supervision; B.A.A, P.C.O, P.E, A.O, A.S, A.K and J.E.O were involved in project administration; B.A.A, P.C.O, P.E, A.O, A.S, A.K, J.A and J.E.O were involved in funding acquisition.

Data Availability

All data supporting the findings of this study are available within the paper and its Supplementary Information.

References

1. Shrestha R, Ban S, Devkota S, Sharma S, Joshi R, Tiwari AP, Kim HY, Joshi MK. Technological trends in heavy metals removal from industrial wastewater: A review. J Environ Chem Eng. 2021;9:105688. 10.1016/j.jece.2020.105688.
2. Chai WS, Cheun JY, Kumar PS, Mubashir M, Majeed Z, Banat F, Ho SH, Show PL. A review on conventional and novel materials towards heavy metal adsorption in wastewater treatment application. J Clean Prod. 2021;296:126589. 10.1016/j.jclepro.2021.126589.
3. Reta YD, Desissa TD, Desalegn YM. Adsorption of heavy metal ions from wastewater: A critical review. Desalination Water Treat. 2023;315:413–31. 10.5004/dwt.2023.31452.
4. Park CM, Yoon Y. Removal of heavy metals from water sources in the developing world using low-cost materials: A review. Chemosphere. 2019;229:142–59. 10.1016/j.chemosphere.2019.04.169.
5. Rinaudo M. Chitin and chitosan: Properties and applications. Prog Polym Sci. 2006;31(7):603–32. 10.1016/j.progpolymsci.2006.06.001.

6. Younes I, Rinaudo M. Chitin and chitosan preparation from marine sources: Structure, properties and applications. Mar Drugs. 2015;13(3):1133–74. 10.3390/md13031133.
7. Trung TS, Tram LH, Van Tan N, Van Hoa N, Cong Minh N, Thanh Loc P, Stevens WF. Improved method for production of chitin and chitosan from shrimp shells. Carbohydr Res. 2020;489:107913. 10.1016/j.carres.2020.107913.
8. Aranaz I, Mengíbar M, Harris R, Paños I, Miralles B, Acosta N, Galed G, Heras Á. Functional characterization of chitin and chitosan. Curr Chem Biol. 2009;3(2):203–30. 10.2174/187231309788166415.
9. Gamage A, Jayasinghe N, Thiviya P, Wasana MLD, Merah O, Madhujith T, Koduru JR. Recent application prospects of chitosan-based composites for the metal-contaminated wastewater treatment. Polymers. 2023;15:1453. 10.3390/polym15061453.
10. Zhang Y, Zhao M, Cheng Q, Wang C, Li H, Han X, Fan Z, Su G, Pan D, Li Z. Research progress of adsorption and removal of heavy metals by chitosan and its derivatives: A review. Chemosphere. 2021;279:130927. 10.1016/j.chemosphere.2021.130927.
11. Ashraf A, Dutta J, Farooq A, Rafatullah M, Pal K, Kyzas GZ. Chitosan-based materials for heavy metal adsorption: Recent advancements, challenges and limitations. J Mol Struct. 2024;1309:138225. 10.1016/j.molstruc.2024.138225.
12. Kurita K. Chitin and chitosan: Functional biopolymers from marine crustaceans. Mar Biotechnol. 2006;8(3):203–26. https://doi.org/10.1007/s10126-005-0097-5.
13. Kumar PS, Lee JH. Kinetics of cadmium uptake by chitosan-based crab shells. Water Res. 2002;36(13):3219–26. 10.1016/S0043-1354(02)00044-1.
14. Tapia A, Seña R, Zambrano H, Paredes V. Extraction and characterization of chitosan obtained from shells of crab (Callinectes bocourti and Callinectes sapidus). Int J Biol Macromol, 32025; 20(Part 3), Article 145963. https://doi.org/10.1016/j.ijbiomac.2025.145963
15. Adeyemi AO, Ojoawo SO. Production and characterization of chitosan of crustacean shells. Materials Today: Proceedings, 2023; 88(Part 1), 128–134. https://doi.org/10.1016/j.matpr.2023.05.729
16. Kumari S, Kishor R. Chitin and chitosan: Origin, properties, and applications. In S. Gopi, S. Thomas, & A. Pius, editors, Handbook of chitin and chitosan: Volume 1: Preparation and properties, 2020; (pp. 1–33). Elsevier. https://doi.org/10.1016/B978-0-12-817970-3.00001-8
17. Sugiyanti E, Nurjanah S, Djumarti N. Preparation and characterization of chitosan from Indonesian shrimp and crab shell waste. Pakistan J Nutr. 2018;17(9):446–53. https://doi.org/10.3923/pjn.2018.446.453.
18. World Health Organization (WHO). Guidelines for drinking-water quality: Fourth edition incorporating the first, second and third addenda. Geneva: World Health Organization. (World Health Organization),; 2026.
19. Standards, Organisation of Nigeria (SON). Nigerian Standard for Drinking Water Quality (NIS 554:2015). Abuja, Nigeria: Standards Organization of Nigeria. The SON catalogue; 2015.
20. Berhanu KG, Tegegn AM, Aragaw TT, Angualie GS, Yismaw AB. The Secret of the Main Campus Water-Wells, Arba Minch University, Ethiopia. J Environ Public Health 2021 Article 4248505, 9pages. https://doi.org/10.1155/2021/4248505
21. Shube H, Karuppannan S, Haji M, Paneerselvam B, Kawo N, Mechal A, Fekadu A. Appraising groundwater quality and probabilistic human health risks from fluoride-enriched groundwater using the pollution index of groundwater (PIG) and GIS: a case study of Adama town and its vicinities in the central main Ethiopian Rift Valley. RSC Adv. 2024;14:30272–85. https://doi.org/10.1039/D4RA02890B.
22. Lindsey BD, Belitz K, Cravotta CA, Toccalino III, P. L., Dubrovsky NM. Lithium in groundwater used for drinking-water supply in the United States. Sci Total Environ. 2021;767:144691. https://doi.org/10.1016/j.scitotenv.2020.144691.
23. Sharma N, Westerhoff P, Zeng C. Lithium occurrence in drinking water sources of the United States. Chemosphere, 305, 135458. https://doi.org/10.1016/j.chemosphere.2022.135458

Figures

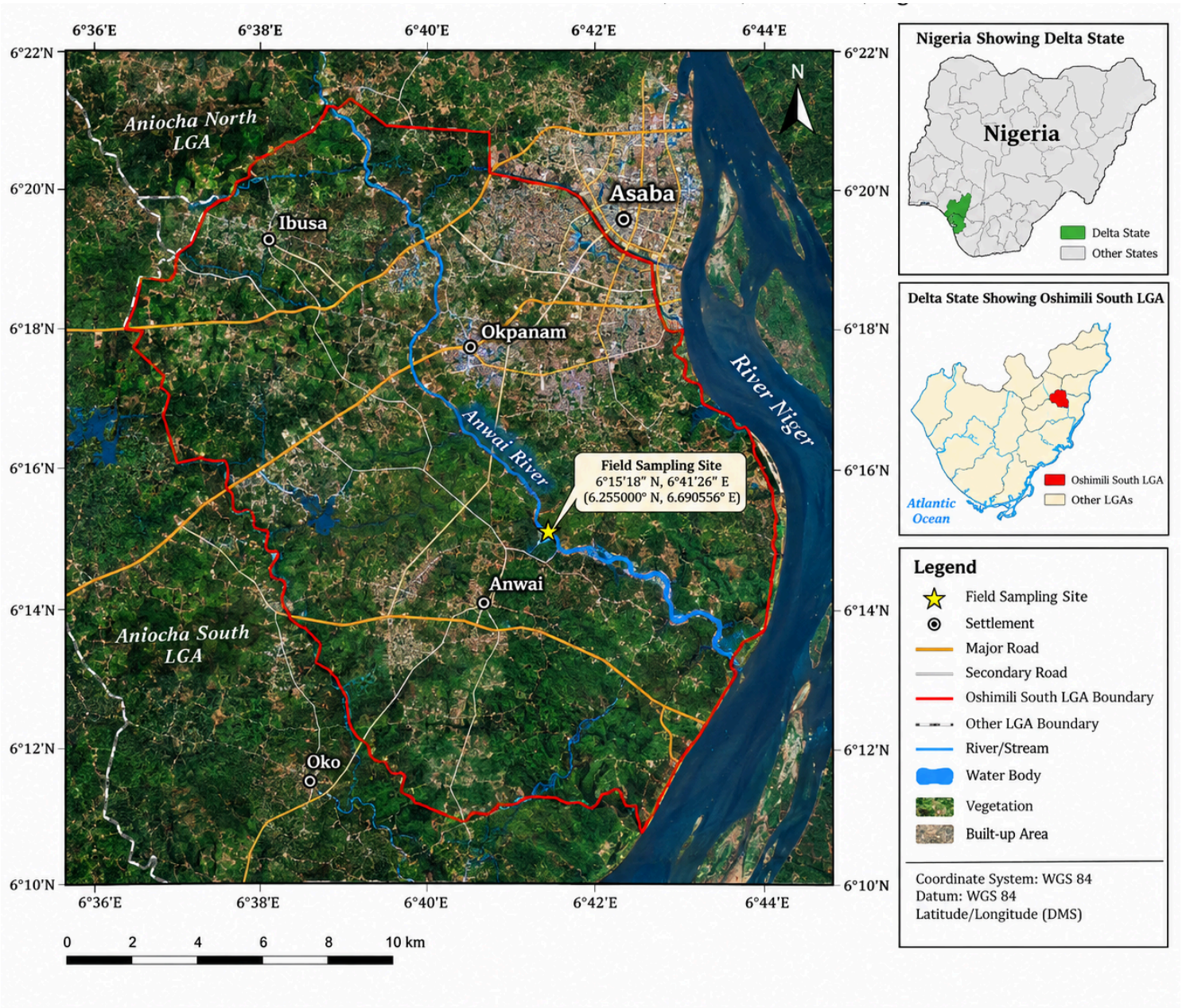


Figure 1

Map location of field sampling site on Anwai River, Oshimil South Local Government Area, Asaba, Delta State, Nigeria

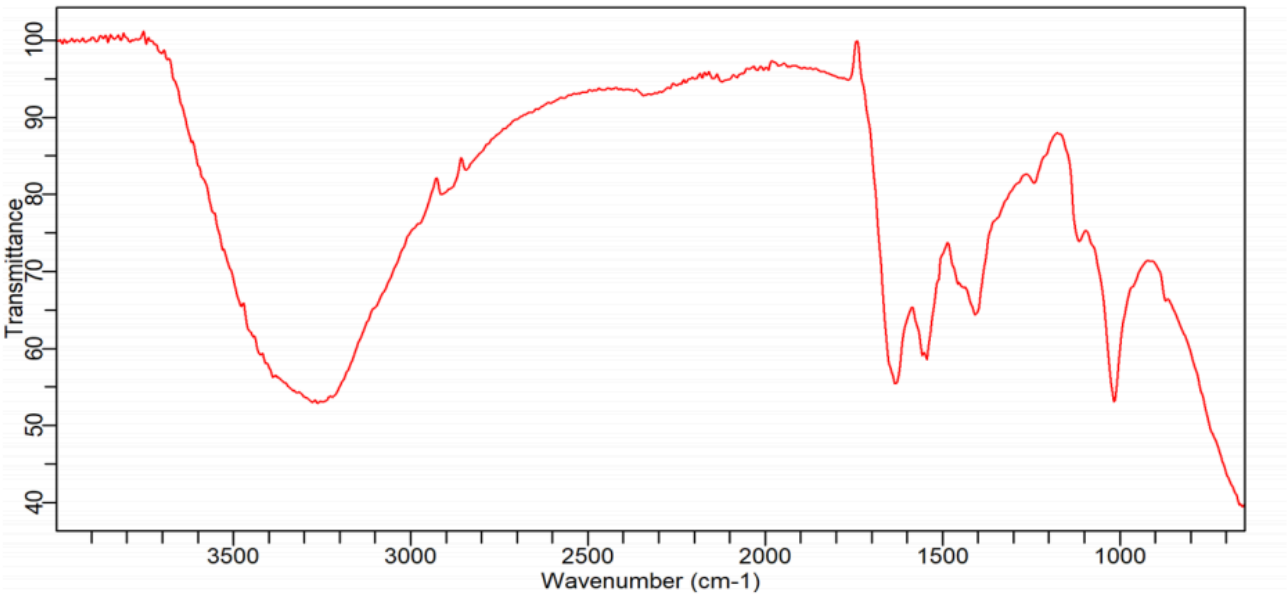


Figure 2

FTIR spectra of Chitin

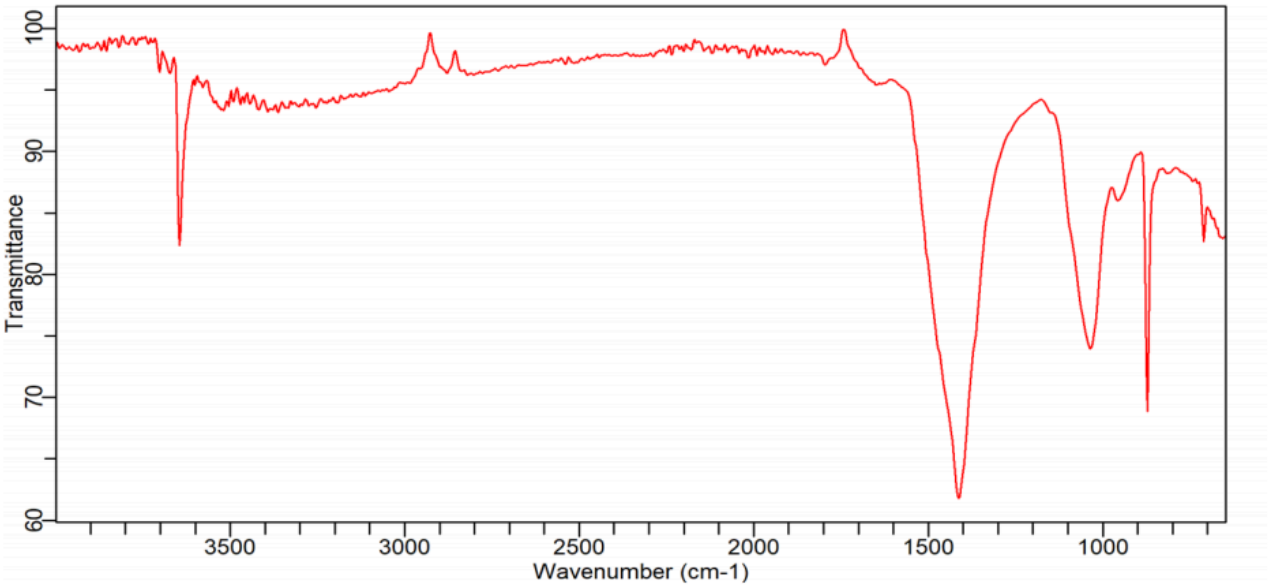


Figure 3

FTIR spectra of Chitosan